Cell Transplantation, Vol. 24, pp. 681–690, 2015
Printed in the USA.

0963-6897/15 $90.00 + .00
DOI: http://dx.doi.org/10.3727/096368915X687769
E-ISSN 1555-3892
www.cognizantcommunication.com

Proof of Concept Studies Exploring the Safety and Functional Activity of Human Parthenogenetic-Derived Neural Stem Cells for the Treatment of Parkinson's Disease

Rodolfo Gonzalez,* Ibon Garitaonandia,* Andrew Crain,† Maxim Poustovoitov,* Tatiana Abramihina,* Alexander Noskov,* Chuan Jiang,‡ Robert Morey,‡ Louise C. Laurent,‡ John D. Elsworth,§¶ Evan Y. Snyder,† D. Eugene Redmond, Jr.,§¶ and Ruslan Semechkin*

*International Stem Cell Corporation, Carlsbad, CA, USA
†Sanford-Burnham Medical Research Institute, La Jolla, CA, USA
‡Department of Reproductive Medicine, UC San Diego, La Jolla, CA, USA
§Axion Research Foundation, Hamden, CT, USA
¶Departments of Psychiatry and Neurosurgery, Yale University School of Medicine, New Haven, CT, USA

Recent studies indicate that human pluripotent stem cell (PSC)-based therapies hold great promise in Parkinson's disease (PD). Clinical studies have shown that grafted fetal neural tissue can achieve considerable biochemical and clinical improvements in PD. However, the source of fetal tissue grafts is limited and ethically controversial. Human parthenogenetic stem cells offer a good alternative because they are derived from unfertilized oocytes without destroying viable human embryos and can be used to generate an unlimited supply of neural stem cells for transplantation. Here we evaluate for the first time the safety and engraftment of human parthenogenetic stem cell-derived neural stem cells (hpNSCs) in two animal models: 6-hydroxydopamine (6-OHDA)-lesioned rodents and 1-methyl-4-phenyl-1,2,3,6-tetrahydropyridine (MPTP)-treated nonhuman primates (NHPs). In both rodents and nonhuman primates, we observed successful engraftment and higher dopamine levels in hpNSC-transplanted animals compared to vehicle control animals, without any adverse events. These results indicate that hpNSCs are safe, well tolerated, and could potentially be a source for cell-based therapies in PD.

Key words: Parthenogenetic stem cells; Neural stem cells (NSCs); Parkinson's disease (PD)

INTRODUCTION

Clinical studies on intrastriatal grafts of human fetal mesencephalic tissue have shown that cell therapy has significant potential for the treatment of Parkinson's disease (PD) (12,15,17,19,20,22). However, there are many concerns associated with using fetal tissue: the source is ethically controversial, and there are practical disadvantages, such as heterogeneity of the tissues and difficulty finding suitable donors (11). Alternatively, recent efforts focused on the use of human pluripotent stem cell (PSC)-derived neural cells and expandable human neural stem cells (NSCs) derived from fetal tissue have shown successful engraftment into the host striatum and improvement in behavioral deficits in animal models of PD (3,16,21,26,35,36). Fetal NSCs have been shown to exhibit migratory ability, paracrine support, and immunomodulating properties that overall promote host repair of the nigrostriatal system (24,26). Here we evaluate for the first time human parthenogenetic stem cell-derived NSCs (hpNSCs) in proof-of-concept studies in two animal models of PD. Human parthenogenetic stem cells (hpSCs) were used as a source of pluripotent stem cells because of their ethical and potential clinical advantages. The ethical basis stems from the fact that hpSCs are derived from unfertilized eggs, avoiding the destruction of a potentially viable human embryo, while clinically they can be made in an HLA homozygous manner, decreasing the chances of immune rejection (29,30). The results of these studies show the successful engraftment of hpNSCs in two animal models.

MATERIALS AND METHODS

Derivation of Human Parthenogenetic Neural Stem Cells (hpNSCs)

hpSC line LLC2P (International Stem Cell Corporation, Carlsbad, CA, USA) (30) was cultured under feeder-free conditions in StemPro hESC SFM supplemented with 8 ng/ml bFGF and 0.1 mM 2-mercaptoethanol on Geltrex Substrate (Life Technologies, Carlsbad, CA,

Received January 13, 2015; final acceptance March 9, 2015. Online prepub date: March 24, 2015.
Address correspondence to Dr. Ruslan Semechkin, International Stem Cell Corporation, 5950 Priestly Drive, Carlsbad, CA 92008, USA.
E-mail: ras@intlstemcell.com

USA). Cells were subcultured with StemPro Accutase (Life Technologies), and when the culture reached 80% confluency, it was treated with 5 μM SB218078 and 1 μM DMH-1 (Tocris, Bristol, UK) in knockout DMEM/F12, 1× GlutaMax, 1× N2/B27 Supplement (Life Technologies) for 11 days. Neuralized hpSCs were dissociated with StemPro Accutase and Y-27632 dihydrochloride (Tocris) and plated on Geltrex-coated dishes in StemPro NSC SFM (Life Technologies). hpNSCs were subcultured for five passages in StemPro NSC SFM before in vitro characterization and in vivo studies.

RNA-Seq Library Construction

RNA was isolated from cells with RNeasy Plus Mini kit (Qiagen, Valencia, CA, USA), quantified with Qubit RNA Assay Kit (Life Technologies) and quality controlled with RNA6000 Nano Kit and BioAnalyzer 2100 (Agilent Technologies, Santa Clara, CA, USA). Approximately 600 ng was used as input for the Illumina TruSeq Stranded mRNA LT Sample Prep Kit (Illumina, Inc., San Diego, CA, USA), and sequencing libraries were created according to the manufacturer's protocol. Briefly, poly-A containing mRNA molecules were purified using poly-dT magnetic beads. After purification, the mRNA was fragmented, and first-strand cDNA was produced using random primers and reverse transcriptase. Second-strand cDNA synthesis was then performed using DNA polymerase I and RNase H. The cDNA was then ligated to indexed Illumina adapters and enriched with PCR to create the cDNA library. The library was then sequenced on a HiSeq 2000 (Illumina, Inc.) instrument as per manufacturer's instructions with paired-end 2 × 101 cycles of sequencing.

RNA-Seq Data Processing

First, 12 bases were trimmed from the 5 end of each read using FASTX (version 0.0.13) (Cold Spring Harbor Laboratory, Cold Spring Harbor, NY, USA). The adaptors were then trimmed using Trim Galore (version 0.2.2; Babraham Institute, Cambridgeshire, UK) and mapped to the hg19 reference genome using TopHat (version 2.0.6; Johns Hopkins University, Baltimore, MD, USA). Samtools (version 0.1.17; Welcome Trust Sanger Institute, Cambridge, UK) was then used to sort, merge, and eliminate duplicate reads. We obtained an average of 18,732,804 mapped reads for the three hpSC samples and 29,666,190 mapped reads for the three NSC samples. Expression levels for each gene were quantified using the Python script rpkmforgenes (25) (Karolinska Institutet, Stockholm, Sweden) and annotated using RefSeq (archive-2012-03-09-03-24-410; National Center for Biotechnology Information, Bethesda, MD, USA). Genes that did not have at least one sample with at least five reads were removed from the analysis. The data was then normalized using the R (version 3.0.1) package DESeq (version 1.12.0; The R Foundation for Statistical Computing, Vienna, Austria) (1). Differential expression analysis and heat maps were done using Qlucore Omics Explorer 2.3 (Qlucore AB, Lund, Sweden). The transcripts were first filtered using a variance filter of 0.1, and then a *t*-test ($q < 0.01$) was performed to identify transcripts that were differentially expressed between the NSCs and the hpSCs. DAVID (National Cancer Institute, Frederick, MD, USA) (18) was used for functional enrichment analysis. Sequencing data is available at the NCBI GEO database (National Center for Biotechnology Information) under the accession designation GSE52912.

RT-PCR Analysis

Total RNA was isolated using RNeasy Plus Mini kit, according to the manufacturer's instructions (Qiagen). Total RNA was used for reverse transcription with the iScript cDNA synthesis kit (Bio-Rad, Irvine, CA, USA) and Px2 Thermal Cycler (Thermo Scientific, Waltham, MA, USA). To analyze gene expression, PCR reactions were performed in triplicate using 1/25th of the cDNA per reaction and the QuantiTect Primer Assay and Quantitest SYBR Green master mix (Qiagen). qPCR was performed using the Rotor-Gene Q (Qiagen) 5 min at 95°C, 5 s at 92°C, and 20 s at 60°C for 37 cycles followed by melting to check the specificity of the amplicons from 50°C to 99°C raising by 1°C each step. Relative quantification was performed against a standard curve, and quantified values were normalized against the input determined by PPIG. The primers used for the analysis are listed in Table 1.

Flow Cytometry

For flow cytometry analysis, samples were harvested with StemPro Accutase (Life Technologies), washed with DPBS (Life Technologies), and fixed with 4% paraformaldehyde (Affymetrix, Santa Clara, CA, USA) for 30 min at room temperature. Cells were washed twice with PBS and blocked for 1 h at room temperature with 0.3% Triton X-100 (Sigma-Aldrich, St. Louis, MO, USA), 5% normal donkey serum (Millipore, Temecula, CA, USA), and 1% BSA (Sigma-Aldrich) in PBS. Cells were then incubated overnight at 4°C with primary antibody in 0.3% Triton X-100, 5% normal donkey serum, and 1% BSA in PBS. Cells were washed twice with PBS and incubated for 1 h at room temperature with secondary antibody in 0.3% Triton X-100, 5% normal donkey serum, and 1% BSA in PBS. The samples were run and analyzed on a Becton Dickinson C6 Accuri Cytometer (BD Biosciences, San Jose, CA, USA). The antibodies used are listed in Table 2.

hpNSC Transplantation in Rodents

Adult male Sprague–Dawley rats (Charles River Laboratories, San Diego, CA, USA) with unilateral,

Table 1. RT-PCR Primers

Gene	Catalog No.	Manufacturer
MSI1	QT00025389 QuantiTect Primer Assay	Qiagen
NES	QT00235781 QuantiTect Primer Assay	Qiagen
PAX6	QT00071169 QuantiTect Primer Assay	Qiagen
POU5F1	QT00210840 QuantiTect Primer Assay	Qiagen
SOX1	QT01008714 QuantiTect Primer Assay	Qiagen
SOX2	QT00237601 QuantiTect Primer Assay	Qiagen
SOX3	QT00212212 QuantiTect Primer Assay	Qiagen
NANOG	QT01844808 QuantiTect Primer Assay	Qiagen
PPIG (Cyclophilin G)	QT01676927 QuantiTect Primer Assay	Qiagen

medial forebrain bundle 6-hydroxydopamine (6-OHDA) (Sigma-Aldrich) lesions of the nigrostriatal pathway were immunosuppressed by daily oral administration of 15 mg/kg of cyclosporine A (Sigma-Aldrich) and reduced to 10 mg/kg per day after 60 days. After 6-OHDA lesion, a burr hole was drilled over the target area, and 5×10^5 hpNSC cells (10 rats) or vehicle (DPBS) (Life Technologies) control (six rats) were injected into the striatum following stereotactic coordinates, divided into two sites at coordinates relative to bregma and dura: anterior–posterior (AP) +1 mm, mediolateral (ML) +2.6 mm, dorsoventral (DV) −4.5 and −5.5 mm, with the incisor bar set at +2.5 mm. A total of 2.5 µl of the cell suspension was injected per site (100,000 cells/µl) at a rate of 1 µl/min over a period of 15 min. All procedures were done following the National Institutes of Health (NIH) Guide for the Care and Use of Laboratory Animals and were approved by the Institutional Animal Care and Use Committee (IACUC) of Explora BIOLABS (San Diego, CA, USA).

Tissue Processing in Rodents

Twenty-eight weeks after transplantation, rats received overdoses of isoflurane (Baxter, Deerfield, IL, USA) to induce deep anesthesia, blood was collected from each animal, and brains were transcardially perfused at a rate 2.5–3 ml/min with ice-cold PBS (heparinized) (Sigma-Aldrich) followed by 4% paraformaldehyde (PFA) (Sigma-Aldrich). Brains were then extracted, postfixed in 4% PFA for 4 h, and soaked in 20% sucrose solution (Sigma-Aldrich) overnight for equilibration. Brains were embedded in Tissue-Tek OCT Compound (VWR, Visalia, CA, USA), frozen at −80°C, and sectioned in a cryostat. Then, 10 µm coronal sections were mounted onto charged slides and frozen at −80°C.

Table 2. Antibodies

Antigen	Catalog No.	Dilution	Application	Manufacturer
TUBB3	MBR-435P	1:500	IHC	Covance
MSI1	ab52865	1:300	ICC	Abcam
	561468	1:20	Flow cytometry	BD Biosciences
NES	ab6320	1:200	ICC	Abcam
	ab6320	1:100	IHC	Abcam
	561231	1:20	Flow cytometry	BD Biosciences
SOX2	ab79351	1:100	ICC	Abcam
	561506	1:20	Flow cytometry	BD Biosciences
CD133	130-098-825	1:20	Flow cytometry	Miltenyi Biotec
TH	P60101-0	1:500	IHC	Pel-Freeze
STEM121	AB-121-U-050	1:500	IHC	Stem Cells, Inc.
GFAP	ab7260	1:1,000	IHC	Abcam
IBA-1	P40101-0	1:200	IHC	Pel-Freeze
Ki-67	ab15580	1:100	IHC	Abcam
OCT-4	ab19857	1:500	IHC	Abcam
	561628	1:20	Flow cytometry	BD Biosciences
SSEA-4	561565	1:20	Flow cytometry	BD Biosciences
GIRK2	ab30838	1:200	IHC	Abcam
VMAT2	AB1598P	1:300	IHC	Millipore
Synaptophysin	1870	1:300	IHC	Epitomics

Biochemical Assays in Rodents

Whole rat brain tissue was weighed, homogenized, normalized for volume, and analyzed for quantitative determination of DA using a commercial ELISA assay kit following the manufacturer's instructions (Cusabio, Wuhan, P. R. China). Brain-derived neurotrophic factor (BDNF) and glial-derived neurotrophic factor (GDNF) levels were also measured in homogenized rat brain tissue by ELISA according to the manufacturer's protocols (Abcam, Cambridge, UK). Data measurement and analysis was performed using the microtiter plate reader BioTek Synergy 2 (BioTek, Winooski, VT, USA).

Detection of Human Cells in Rodent Tissue

Detection of engrafted human cells was done according to a previously published protocol with some modifications (32). Genomic DNA was isolated from portions of homogenized rat brain hemispheres and organs with DNeasy Blood & Tissue kit (Qiagen) according to the manufacturer's protocol and was quantified with Quant-iT dsDNA Assay kit (Life Technologies). Primers used in the reaction are from the -satellite DNA on human chromosome 17, previously described by Becker et al. (2), and the sequences are: 5 -GG G ATA ATT TCA GCT GAC TAA ACA G-3 and 5 -AAA CGT CCA CTT GCA GAT TCT AG-3 . The PCR reaction mixture contained 2× Rotogene SYBR green PCR Master mix (Qiagen), 250 nM of each primer, and genomic DNA template. The reactions were performed with the Rotor-Gene Q (Qiagen) with the following cycling conditions: 5 min at 95°C, 5 s at 92°C, and 20 s at 60°C for 37 cycles followed by high-resolution melting from 50°C to 99°C raising by 0.1°C each step. Standard curve was built with serial dilutions of human genomic DNA from 5 ng up to 0.000005 ng per reaction. Serial dilutions were prepared using rat genomic DNA, so total DNA load per reaction was 10 ng. Assuming one human cell has approximately 3 pg of genomic DNA, standard curves demonstrated that the assay detected a single human cell in a background of 2×10^5 rodent cells. The calculation of human DNA content in the rat brains was based on the standard curve and normalized against a sample of rat brain hemisphere spiked with 500,000 human cells.

MPTP Administration and Immunosuppression in Nonhuman Primates

Two adult male St. Kitts/African green monkeys (*Chlorocebus sabaeus*) were housed at the St. Kitts Biomedical Research Foundation facility, where they were singly housed with a natural daylight light/dark cycle at 17° north latitude. The animals received food and water ad libitum or were supplemented with special feeding, if needed, during the course of the study. The monkeys were systematically treated with standard doses of 1.2 mg/kg of 1-methyl-4-phenyl-1,2,3,6-tetrahydropyridine (MPTP; Sigma-Aldrich) via intramuscular (IM) injections administered over a 5-day period to induce bilateral degeneration of the nigrostriatal pathway (7,9). MPTP produces toxic effects with a high degree of specificity for the DA system. Monkeys were immunosuppressed 1 day prior to grafting and continued until sacrifice with a triple drug immunosuppression regimen of 1 mg/kg/day cyclosporine A (Sandimmune; Henry Schein Animal Health, Pittsburgh, PA, USA), 0.6 mg/kg/day prednisone (Sandimmune; Henry Schein Animal Health), and 1 mg/kg/day azathioprine (Sigma-Aldrich) (26).

Transplantation of hpNSCs Into Nonhuman Primate Brains

The two MPTP-lesioned asymptomatic adult African green monkeys were transplanted unilaterally with 8 million hpNSCs into four different sites: anterior caudate nucleus, posterior caudate nucleus, putamen, and substantia nigra. The cellular suspension was drawn into a 22-gauge needle connected to a Hamilton syringe (Hamilton, Reno, NV, USA) immediately prior to implantation into the target sites, which were verified using standard stereotactic procedures and coordinates from ear bar zero: AP +23.9 mm, lateral +3.5 mm, vertical +18.6 mm (anterior caudate nucleus); AP +19.9 mm, lateral +3.5 mm, vertical +18.6 mm (posterior caudate nucleus); AP + 21.9 mm, lateral +10 mm, vertical +18.6 mm (putamen); AP +11.1 mm, lateral +3.5 mm, vertical +12.1 mm (substantia nigra). Insertion was performed slowly over a 2-min period, and the tip of the needle was permitted to remain in the implantation site for at least 2 min prior to injection. Cells were extruded using a controlled perfusion pump (Stoelting, Wood Dale, IL, USA) at a maximum rate of 1 µl/min, with a 2-min delay before cannula withdrawal at a rate of 1 mm/min for 5 mm and then slowly until out of the brain. A total of 10 µl of the cell suspension containing 200,000 cells/µl was injected per site. The study was performed in accordance with US federal guidelines and with approval of the IACUC of Axion Research Foundation.

Tissue Processing in Nonhuman Primates

Monkeys were sacrificed 14 weeks following hpNSC transplantation using ketamine (8-10 mg/kg, IM) (Sigma-Aldrich) and sodium pentobarbital (30–100 mg/kg, IV, or more until loss of deep corneal reflex) (Sigma-Aldrich). The brains were removed after transcardial perfusion with ice-cold heparinized saline and postfixed in 4% paraformaldehyde in 0.1 M phosphate buffer (pH 7.4) (Sigma-Aldrich) for 24 h, followed by storage in PBS. Prior to postfixation, brains were sliced into 4-mm coronal sections using a custom-made brain mold.

Dopamine Analysis in Nonhuman Primates

Tissue punches were removed with a stainless steel punch (1.2 mm diameter) and frozen in liquid nitrogen as previously described (7,8). The concentration of dopamine

was determined by HPLC by modification of previously published methods, which allows the detection limit of 5–10 fmol DA (7,8). Tissue concentrations of dopamine were corrected for the amount of protein in the sample analyzed.

Immunohistochemistry

Brain sections were washed in Tris buffer (0.1 M Tris, 085% NaCl, pH 7.5) for 5 min and incubated for 20 min in 3% H_2O_2, 10% methanol in Tris buffer (Sigma-Aldrich). The sections were then washed for 5 min in Tris buffer, 15 min in wash buffer (0.1% Triton X-100 in Tris buffer), and 15 min in blocking buffer (2% BSA, 0.1% Triton X-100 in Tris buffer) (Sigma-Aldrich). Sections were incubated with primary antibody diluted in blocking buffer at room temperature overnight with shaking. Sections were washed for 15 min in wash buffer and 15 min in blocking buffer, and incubated for 1 h at room temperature with secondary antibody diluted in blocking buffer. Sections were washed four times, and coverslips were mounted on the slides with mounting medium containing DAPI (Sigma-Aldrich). Antibodies used are described in Table 2.

Statistical Analysis

Data are presented as mean ± standard error of mean (SEM). Statistical analyses were performed using a confidence level of 95% (= 0.05) with two-tailed Student's

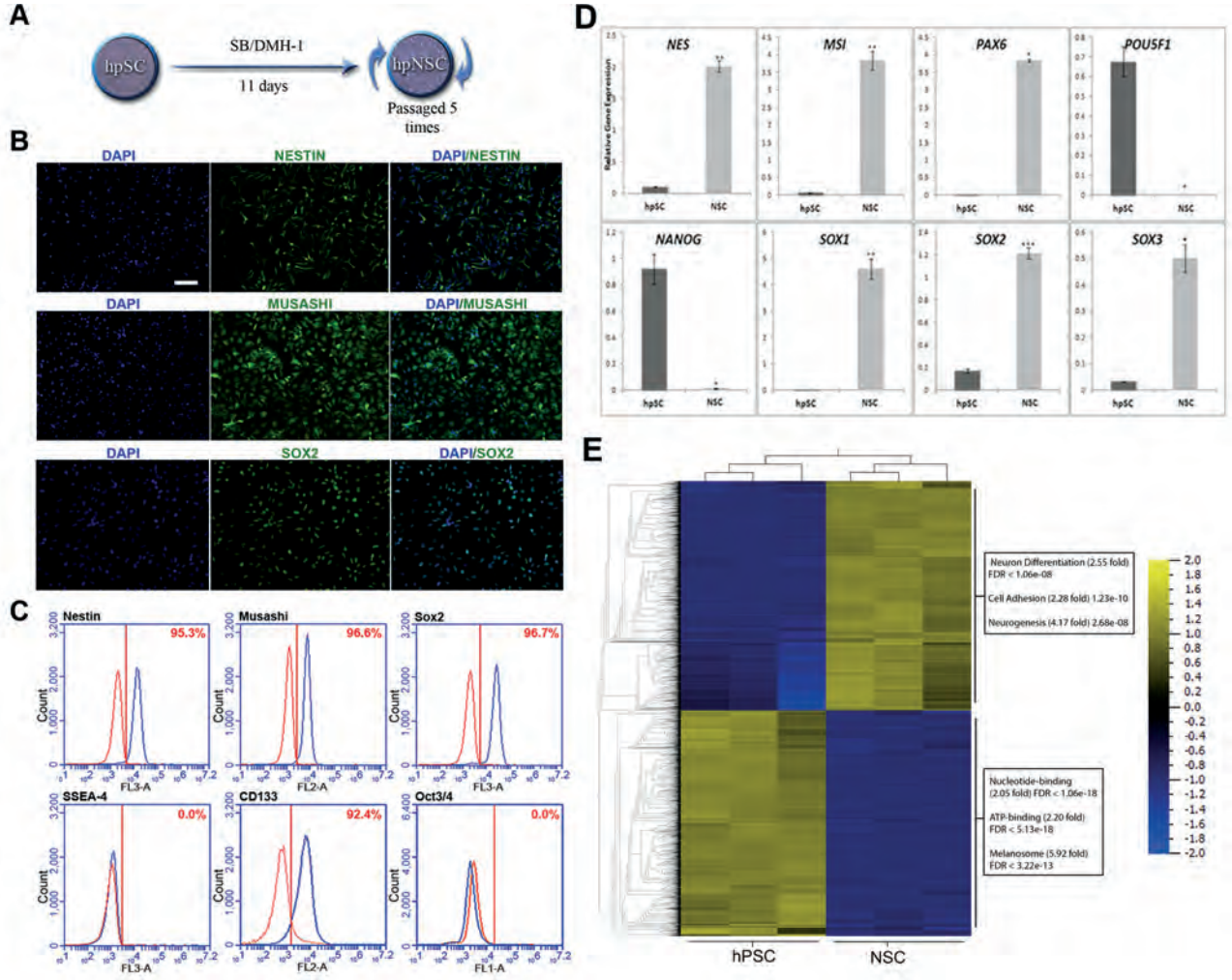

Figure 1. Derivation and characterization of hpNSCs. (A) Flow diagram of differentiation of hpSCs into hpNSCs. (B) Immunocytochemical analysis of hpNSCs for NSC markers Nestin, SOX2, and Musashi. (C) FACS analysis of hpNSCs for Nestin, Musashi, SOX2, CD133, and pluripotency markers OCT-4 and SSEA-4. Percentage of positive cells (blue) is calculated based on isotype control stained cells (red). (D) Gene expression analysis of hpNSCs compared to pluripotent hpSCs ($n = 3$). (E) Functional enrichment analysis was performed using DAVID Bioinformatics Resources Functional Annotation Tool. The most significant enrichments for the top annotation clusters, with their FDRs, are shown for the two sets of differentially expressed genes (the set that was more highly expressed in hPSCs, and the set that was more highly expressed in NSCs). Scale bar: 100 μm.

t-test. The statistical analyses were performed with GraphPad Prism (GraphPad Software, La Jolla, CA, USA). The criterion for statistical significance for all tests was $p < 0.05$ (*$p < 0.05$; **$p < 0.01$; ***$p < 0.001$).

RESULTS

Generation and Characterization of hpNSCs

The generation of hpNSCs was performed under feeder-free conditions with a small molecule inhibitor of bone morphogenic protein (DMH-1) and an inhibitor of checkpoint kinase 1 (SB218078) as previously described (14) (Fig. 1A). hpNSCs were characterized by their expression of NSC markers Nestin, Musashi-1, SOX2, and CD133, a characteristic surface marker (6,34), and the absence of pluripotency markers OCT-4 (POU5F1) and SSEA-4 (Fig. 1B, C). Gene expression analysis using qRT-PCR and RNA-Seq also revealed significant upregulation of neural markers in NSCs compared to undifferentiated hpSCs and a complete downregulation of pluripotency markers *POU5F1* and *NANOG* (Fig. 1D, E). Transcripts that were upregulated in hpNSCs compared to hpSCs showed enrichment for genes involved in neuron differentiation, cell adhesion, and neurogenesis (Fig. 1E).

Transplantation of hpNSCs Into 6-OHDA-Lesioned Rats

Following cell transplantation of hpNSCs into the striatum of 6-OHDA-lesioned rats, animals survived the surgery, gained weight, did not show abnormal behavior other than parkinsonism, and had no tumors for the entire 28-week study period. Postmortem, gross necropsy and histopathology analysis revealed the absence of ectopic tissue, tumors, or hyperproliferation (Table 3). Biodistribution analysis also demonstrated the absence of human cells in peripheral organs (Table 4). Biochemical analysis of brain tissue samples showed that animals grafted with hpNSCs had significantly higher DA levels than vehicle control animals (Fig. 2A). hpNSCs survived and successfully engrafted 28 weeks posttransplantation. Most of the engrafted hpNSCs were dispersed from the graft site and remained undifferentiated, possibly providing neurotrophic support to the nigrostriatal system. Analysis of brain tissue showed a significantly higher level of neurotrophic cytokines BDNF and GDNF in hpNSC-transplanted animals than vehicle control animals (Fig. 2B). Even though the increase in DA and cytokine levels was significant, it is expected that these levels are lower than in unlesioned animals. Dispersed hpNSCs did not appear to elicit a pronounced immune response as evidenced by the low levels of IBA-1$^+$ host microglia and the GFAP$^+$ astrocyte numbers (Fig. 2C). Additionally, differentiation of hpNSCs into DA neurons was observed as shown by the colocalization of the human-specific marker STEM121 with the dopaminergic markers tyrosine hydroxylase (TH), G-protein-regulated inward-rectifier potassium channel 2 (GIRK2), and vesicular monoamine transporter 2 (VMAT2) (Fig. 2D).

Table 3. Gross Necropsy Results in Rodents

Tissue	Description of Finding
Cervical lymph node	N
Salivary gland	N
Thyroid with parathyroid	N
Esophagus, trachea, larynx, tongue	N
Diaphragm	N
Ovaries	N
Uterus	N
Spleen	N
Pancreas	N
Liver	N
Adrenal	N
Kidney	N
GI: stomach, duodenum, jejunum, ileum, cecum, colon, rectum, mesenteric lymph node	N
Urinary bladder	N
Thymus	N
Heart	N
Lung	N

N, normal tissue.

Transplantation of hpNSCs Into MPTP-Treated Nonhuman Primates

To evaluate the effects in a larger PD animal model, hpNSCs were transplanted into MPTP-treated monkeys (28). Biochemical analysis of brain tissue samples showed that animals grafted with hpNSCs had higher DA levels than vehicle control animals (Fig. 3A). hpNSC-transplanted primates had no adverse events, such as dyskinesia, deformations, or tumors, indicating that the transplanted cells were safe and well tolerated by the experimental animals (Fig. 3B). Most importantly, the presence of undifferentiated, pluripotent, OCT-4-positive cells was not detected in any of the grafts (Fig. 3C). hpNSCs survived 14 weeks posttransplantation, dispersed from the graft site, and appeared to have minimal glial scarring (GFAP) or host microglia (IBA-1) surrounding

Table 4. Biodistribution of hpNSC in Rodents

Organs Analyzed	Rats Transplanted With hpNSCs	Sham Control Rats
Liver	N.D.	N.D.
Kidney	N.D.	N.D.
Heart	N.D.	N.D.
Spleen	N.D.	N.D.
Lung	N.D.	N.D.

N.D., not detected.

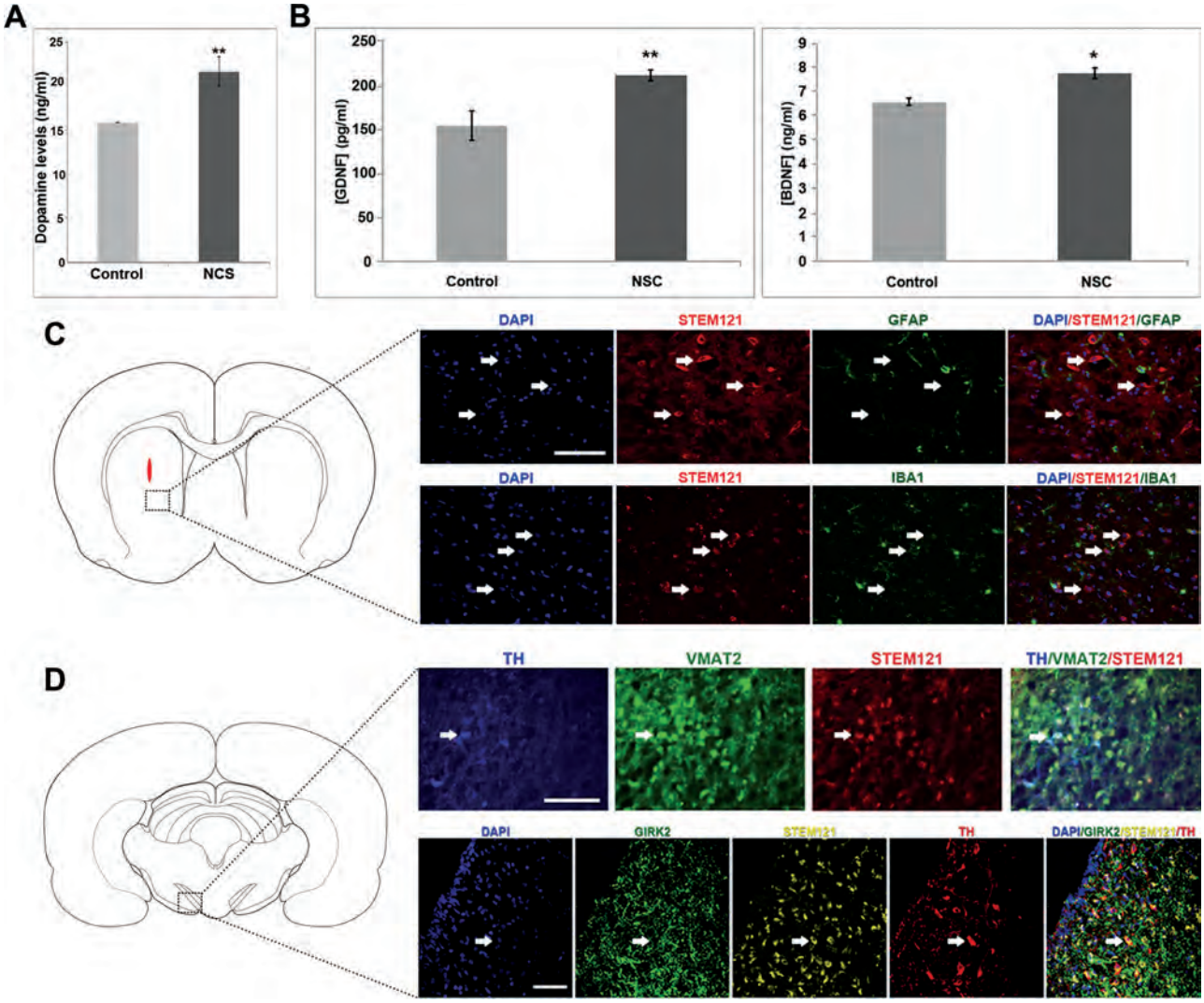

Figure 2. Survival and engraftment of hpNSCs in 6-OHDA-lesioned rats. (A) Higher brain DA levels in hpNSC-transplanted animals versus vehicle control (PBS) rats ($n = 4–8$). (B) GDNF and BDNF levels in homogenized brains of hpNSC and vehicle control transplanted animals ($n = 4–8$). (C) Schematic showing the coronal section of the rat striatum. The red dot represents the site of injection, and the dotted square shows the site where the micrographs were taken in the striatum. Right panels show the micrographs for immunohistochemistry with DAPI (blue), STEM121 (red), astrocytes (GFAP, green), and microglia (IBA-1, green). White arrows point to the engrafted hpNSCs. (D) Schematic showing coronal section of the rat substantia nigra with a dotted square representing the site where the micrographs were taken. On the right are the micrographs showing coexpression, pointed by white arrows, of STEM121 (red) with TH (blue), VMAT2 (green) (top), and STEM121 (yellow), with GIRK2 (green), TH (red), and DAPI (blue) (bottom). Scale bar: 100 μm.

the engrafted hpNSCs (Fig. 3D, E). The majority of the engrafted hpNSCs remained undifferentiated ($Nestin^+$) (Fig. 3F), as previously reported for human NSCs (4,24), and were found in close contact with host DA neurons in the substantia nigra (Fig. 3G), possibly promoting host neural repair by the secretion of neurotrophic factors. As observed in the rodents, we also found evidence of hpNSCs differentiating into DA neurons expressing TH, GIRK2, VMAT2, and synaptophysin (SYP) (Fig. 3H).

DISCUSSION

Previous proof-of-concept studies with human fetal dopamine grafts have showed efficacy in preclinical PD models (5,23,27). Results from the preclinical studies provided a clear indication that grafted fetal dopaminergic neurons could be therapeutically effective and clinical studies followed. The results of the clinical studies showed that grafted fetal dopaminergic neurons could survive and function for more than 10 years in

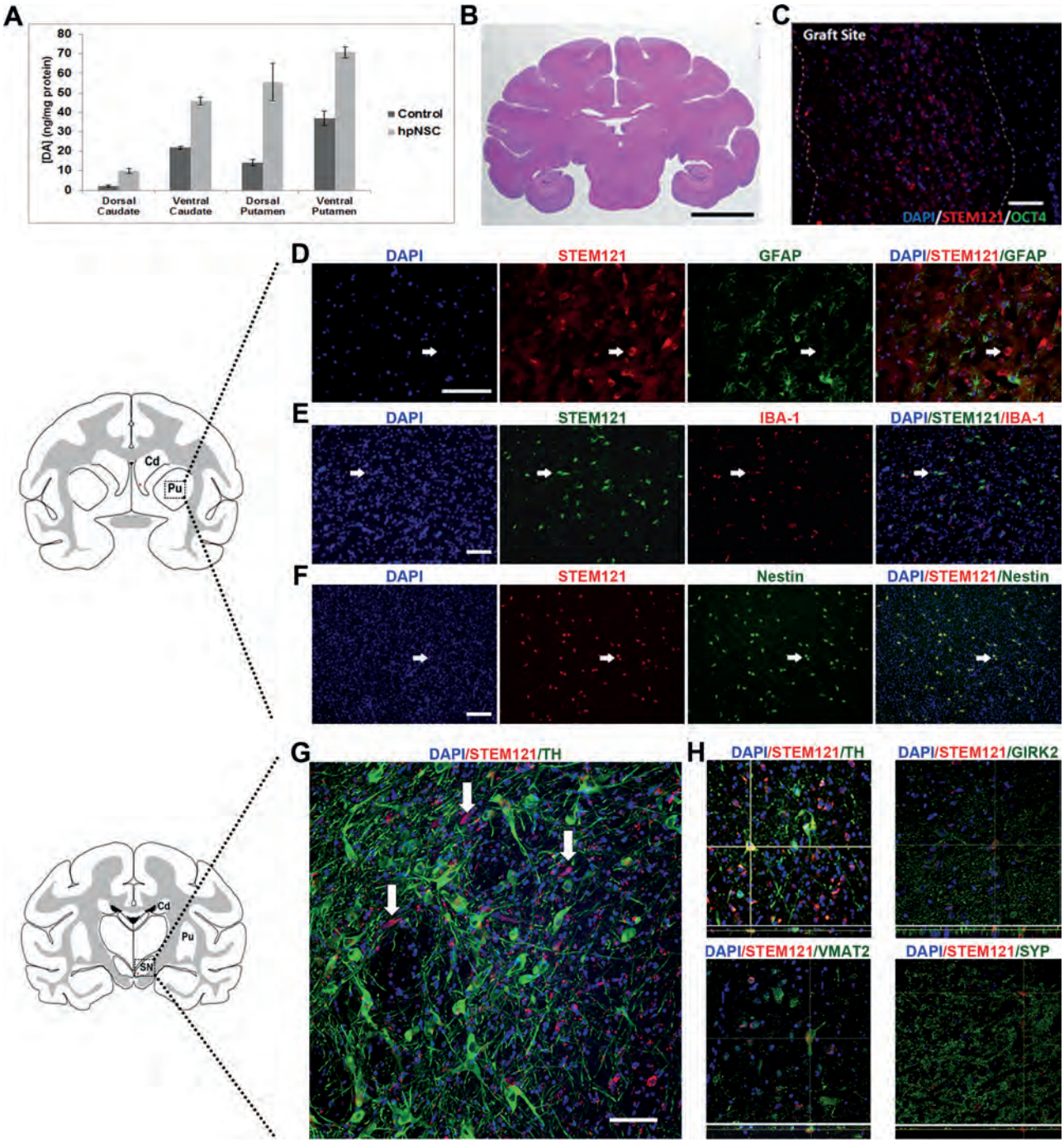

Figure 3. Survival and engraftment of hpNSCs in MPTP-lesioned monkeys. (A) Dopamine levels in different regions of the striatum in hpNSC-transplanted animals compared to historical vehicle control animals ($n = 2$). (B) Representative H&E staining of transplanted monkey brain showing the lack of tumors or ectopic neuroectoderm tissue. (C) Representative staining of the grafted area with human-specific antibody STEM121 (red) and pluripotency marker antibody OCT-4 (green) showing the lack of undifferentiated pluripotent stem cells within the graft. White lines mark the border between the graft and the host. (D, E) Immunohistochemistry for STEM121, GFAP (green), IBA-1 (red), and DAPI (blue). White arrows point to engrafted hpNSCs. Schematic showing coronal section of monkey striatum with a dotted square representing the site where the micrographs were taken. (F) Coexpression, pointed by white arrow, of STEM121 (red), Nestin (green), and DAPI (blue) showing that the majority of hpNSCs remain undifferentiated. (G) Immunohistochemistry for STEM121 (red), TH (green), and DAPI (blue) in the substantia nigra. White arrows point to hpNSCs in close proximity to host DA neurons. (H) Coexpression, indicated by yellow lines, of STEM121 (red) with TH (green), GIRK2 (green), VMAT2 (green), SYP (green), and DAPI (blue). Cd, caudate; Pu, putamen; SN, substantia nigra; Red dots, sites of injection. Scale bars: 1 cm (B) and 100 μm (C–H).

the striatum of some PD patients (15,19). The source of human fetal dopaminergic tissue is limited and clinically impractical. Recent efforts have focused on the use of expandable sources, such as human pluripotent stem cells (PSCs), including human embryonic and induced PSCs. PSC-derived DA neurons successfully engraft into the host striatum and improve behavioral deficits in animal models of PD, by cell replacement and dopamine secretion (16,21,35). A second source of expandable cells is human NSCs derived from fetal tissue, which are scalable and have shown efficacy in preclinical PD models, by paracrine effects (24,26,36).

In this study, we evaluated a third expandable source of cells for therapy, hpNSCs. hpNSCs are particularly attractive for cell therapy because they can be derived in a homozygous manner from heterozygous donors, permitting the creation of cells banks that could potentially match significant segments of the population with only a few cell lines. Here we show for the first time the successful engraftment and safety of hpNSCs following transplantation in rodent and nonhuman primate PD models. In both animal models, transplantation of hpNSCs led to improvement of DA levels, which could be explained by the multimodal actions of NSCs, including neuroprotection, cell replacement, and immunomodulation (26,33). Nonhuman primates transplanted with hpNSCs remained healthy with no abnormal behaviors, such as dyskinesia, a side effect previously observed with human fetal tissue transplants (12). Additionally, we did not detect overgrowth, deformations, or tumors in any of the transplanted animals, contrary to other studies with PSC-derived neural cells (13,31). Postimplantation, hpNSCs survived, dispersed from the graft site, and elicited a low immune response. The immunological response can compromise the survival of the grafts and be a significant barrier to evaluate the outcome to intracerebral transplantation of PSC derivatives (10,21). Higher cytokine levels following transplantation of hpNSCs indicate that hpNSCs could have promoted neural repair of the host nigrostriatal system (3,24,37). Overall, we show for the first time successful engraftment following transplantation of hpNSCs in experimental models of PD and subsequent functional studies following hpNSC transplantation would reveal their potential use as a treatment of PD.

ACKNOWLEDGMENTS: We thank the staff of St. Kitts Biomedical Research Foundation for care and observations of the monkeys, especially C.R. Wilson and X. Morton. C.J. was supported by a CIRM Bridges award to California State University, Channel Islands. R.M. and L.C.L. were supported by funds from the UCSD Department of Reproductive Medicine and CIRM TR3-05603. R.G. and I.G.: conception and design, collection and/or assembly of data, data analysis and interpretation, manuscript writing; A.C., M.P., T.A., A.N., C.J., R.M., L.C.L., J.E., E.S.: collection and/or assembly of data; D.E.R. and R.S.: conception and design, data analysis and interpretation, manuscript writing, final approval of manuscript. All authors who are employees of International Stem Cell Corporation declare this affiliation. In addition, R.S. declares stock ownership. D.E.R. is a paid consultant to International Stem Cell Corporation. A.C., C.J., R.M., L.C.L., J.E., and E.S. declare no conflicts.

REFERENCES

1. Anders, S.; Huber, W. Differential expression analysis for sequence count data. Genome Biol. 11(10):R106; 2010.
2. Becker, M.; Nitsche, A.; Neumann, C.; Aumann, J.; Junghahn, I.; Fichtner, I. Sensitive PCR method for the detection and real-time quantification of human cells in xenotransplantation systems. Br. J. Cancer 87(11):1328–1335; 2002.
3. Bjugstad, K. B.; Teng, Y. D.; Redmond, D. E., Jr.; Elsworth, J. D.; Roth, R. H.; Cornelius, S. K.; Snyder, E. Y.; Sladek, J. R., Jr. Human neural stem cells migrate along the nigrostriatal pathway in a primate model of Parkinson's disease. Exp. Neurol. 211(2):362–369; 2008.
4. Borlongan, C. V.; Fournier, C.; Stahl, C. E.; Yu, G.; Xu, L.; Matsukawa, N.; Newman, M.; Yasuhara, T.; Hara, K.; Hess, D. C.; Sanberg, P. R. Gene therapy, cell transplantation and stroke. Front. Biosci. 11:1090–1101; 2006.
5. Brundin, P.; Strecker, R. E.; Gage, F. H.; Lindvall, O.; Bjorklund, A. Intracerebral transplantation of dopamine neurons: Understanding the functional role of the mesolimbocortical dopamine system and developing a therapy for Parkinson's disease. Ann. N Y. Acad. Sci. 537:148–160; 1988.
6. Cummings, B. J.; Uchida, N.; Tamaki, S. J.; Salazar, D. L.; Hooshmand, M.; Summers, R.; Gage, F. H.; Anderson, A. J. Human neural stem cells differentiate and promote locomotor recovery in spinal cord-injured mice. Proc. Natl. Acad. Sci. USA 102(39):14069–14074; 2005.
7. Elsworth, J. D.; Deutch, A. Y.; Redmond, D. E., Jr.; Taylor, J. R.; Sladek, J. R., Jr.; Roth, R. H. Symptomatic and asymptomatic 1-methyl-4-phenyl-1,2,3,6-tetrahydropyridine-treated primates: Biochemical changes in striatal regions. Neuroscience 33(2):323–331; 1989.
8. Elsworth, J. D.; Sladek, J. R., Jr.; Taylor, J. R.; Collier, T. J.; Redmond, D. E., Jr.; Roth, R. H. Early gestational mesencephalon grafts, but not later gestational mesencephalon, cerebellum or sham grafts, increase dopamine in caudate nucleus of MPTP-treated monkeys. Neuroscience 72(2):477–484; 1996.
9. Elsworth, J. D.; Taylor, J. R.; Sladek, J. R., Jr.; Collier, T. J.; Redmond, D. E., Jr.; Roth, R. H. Striatal dopaminergic correlates of stable parkinsonism and degree of recovery in old-world primates one year after MPTP treatment. Neuroscience 95(2):399–408; 2000.
10. Emborg, M. E.; Zhang, Z.; Joers, V.; Brunner, K.; Bondarenko, V.; Ohshima, S.; Zhang, S. C. Intracerebral transplantation of differentiated human embryonic stem cells to hemiparkinsonian monkeys. Cell Transplant. 22(5):831–838; 2013.
11. Freed, C. R. Will embryonic stem cells be a useful source of dopamine neurons for transplant into patients with Parkinson's disease? Proc. Natl. Acad. Sci. USA 99(4):1755–1757; 2002.
12. Freed, C. R.; Greene, P. E.; Breeze, R. E.; Tsai, W. Y.; DuMouchel, W.; Kao, R.; Dillon, S.; Winfield, H.; Culver, S.; Trojanowski, J. Q.; Eidelberg, D.; Fahn, S. Transplantation of embryonic dopamine neurons for severe Parkinson's disease. N. Engl. J. Med. 344(10):710–719; 2001.
13. Ganat, Y. M.; Calder, E. L.; Kriks, S.; Nelander, J.; Tu, E. Y.; Jia, F.; Battista, D.; Harrison, N.; Parmar, M.; Tomishima,

M. J.; Rutishauser, U.; Studer, L. Identification of embryonic stem cell-derived midbrain dopaminergic neurons for engraftment. J. Clin. Invest. 122(8):2928–2939; 2012.
14. Gonzalez, R.; Garitaonandia, I.; Abramihina, T.; Wambua, G. K.; Ostrowska, A.; Brock, M.; Noskov, A.; Boscolo, F. S.; Craw, J. S.; Laurent, L. C.; Snyder, E. Y.; Semechkin, R. A. Deriving dopaminergic neurons for clinical use. A practical approach. Scientific Reports 3(1463):1–5; 2013.
15. Hallett, P. J.; Cooper, O.; Sadi, D.; Robertson, H.; Mendez, I.; Isacson, O. Long-term health of dopaminergic neuron transplants in Parkinson's disease patients. Cell. Rep. 7(6): 1755–1761; 2014.
16. Hargus, G.; Cooper, O.; Deleidi, M.; Levy, A.; Lee, K.; Marlow, E.; Yow, A.; Soldner, F.; Hockemeyer, D.; Hallett, P. J.; Osborn, T.; Jaenisch, R.; Isacson, O. Differentiated Parkinson patient-derived induced pluripotent stem cells grow in the adult rodent brain and reduce motor asymmetry in Parkinsonian rats. Proc. Natl. Acad. Sci. USA 107(36):15921–15926; 2010.
17. Hauser, R. A.; Freeman, T. B.; Snow, B. J.; Nauert, M.; Gauger, L.; Kordower, J. H.; Olanow, C. W. Long-term evaluation of bilateral fetal nigral transplantation in Parkinson disease. Arch. Neurol. 56(2):179–187; 1999.
18. Huang, D. W.; Sherman, B. T.; Lempicki, R. A. Systematic and integrative analysis of large gene lists using DAVID bioinformatics resources. Nat. Protocols 4(1):44–57; 2008.
19. Kefalopoulou, Z.; Politis, M.; Piccini, P.; Mencacci, N.; Bhatia, K.; Jahanshahi, M.; Widner, H.; Rehncrona, S.; Brundin, P.; Bjorklund, A.; Lindvall, O.; Limousin, P.; Quinn, N.; Foltynie, T. Long-term clinical outcome of fetal cell transplantation for Parkinson disease: Two case reports. JAMA Neurol. 71(1):83–87; 2014.
20. Kordower, J. H.; Freeman, T. B.; Snow, B. J.; Vingerhoets, F. J.; Mufson, E. J.; Sanberg, P. R.; Hauser, R. A.; Smith, D. A.; Nauert, G. M.; Perl, D. P.; et al. Neuropathological evidence of graft survival and striatal reinnervation after the transplantation of fetal mesencephalic tissue in a patient with Parkinson's disease. N. Engl. J. Med. 332(17):1118–1124; 1995.
21. Kriks, S.; Shim, J. W.; Piao, J.; Ganat, Y. M.; Wakeman, D. R.; Xie, Z.; Carrillo-Reid, L.; Auyeung, G.; Antonacci, C.; Buch, A.; Yang, L.; Beal, M. F.; Surmeier, D. J.; Kordower, J. H.; Tabar, V.; Studer, L. Dopamine neurons derived from human ES cells efficiently engraft in animal models of Parkinson's disease. Nature 480(7378):547–551; 2011.
22. Mendez, I.; Vinuela, A.; Astradsson, A.; Mukhida, K.; Hallett, P.; Robertson, H.; Tierney, T.; Holness, R.; Dagher, A.; Trojanowski, J. Q.; Isacson, O. Dopamine neurons implanted into people with Parkinson's disease survive without pathology for 14 years. Nat. Med. 14(5):507–509; 2008.
23. Nikkhah, G.; Bentlage, C.; Cunningham, M. G.; Bjorklund, A. Intranigral fetal dopamine grafts induce behavioral compensation in the rat Parkinson model. J Neurosci. 14(6):3449–3461; 1994.
24. Ourednik, J.; Ourednik, V.; Lynch, W. P.; Schachner, M.; Snyder, E. Y. Neural stem cells display an inherent mechanism for rescuing dysfunctional neurons. Nat. Biotechnol. 20(11):1103–1110; 2002.
25. Ramsköld, D.; Wang, E. T.; Burge, C. B.; Sandberg, R. An abundance of ubiquitously expressed genes revealed by tissue transcriptome sequence data. PLoS Comput. Biol. 5(12):e1000598; 2009.
26. Redmond, D. E., Jr.; Bjugstad, K. B.; Teng, Y. D.; Ourednik, V.; Ourednik, J.; Wakeman, D. R.; Parsons, X. H.; Gonzalez, R.; Blanchard, B. C.; Kim, S. U.; Gu, Z.; Lipton, S. A.; Markakis, E. A.; Roth, R. H.; Elsworth, J. D.; Sladek, J. R., Jr.; Sidman, R. L.; Snyder, E. Y. Behavioral improvement in a primate Parkinson's model is associated with multiple homeostatic effects of human neural stem cells. Proc. Natl. Acad. Sci. USA 104(29):12175–12180; 2007.
27. Redmond, D. E., Jr.; Vinuela, A.; Kordower, J. H.; Isacson, O. Influence of cell preparation and target location on the behavioral recovery after striatal transplantation of fetal dopaminergic neurons in a primate model of Parkinson's disease. Neurobiol. Dis. 29(1):103–116; 2008.
28. Redmond, D. E.; Sladek, J. R., Jr.; Roth, R. H.; Collier, T. J.; Elsworth, J. D.; Deutch, A. Y.; Haber, S. Fetal neuronal grafts in monkeys given methylphenyltetrahydropyridine. Lancet 1(8490):1125–1127; 1986.
29. Revazova, E. S.; Turovets, N. A.; Kochetkova, O. D.; Agapova, L. S.; Sebastian, J. L.; Pryzhkova, M. V.; Smolnikova, V. I.; Kuzmichev, L. N.; Janus, J. D. HLA homozygous stem cell lines derived from human parthenogenetic blastocysts. Cloning Stem Cells 10(1):11–24; 2008.
30. Revazova, E. S.; Turovets, N. A.; Kochetkova, O. D.; Kindarova, L. B.; Kuzmichev, L. N.; Janus, J. D.; Pryzhkova, M. V. Patient-specific stem cell lines derived from human parthenogenetic blastocysts. Cloning Stem Cells 9(3):432–449; 2007.
31. Roy, N. S.; Cleren, C.; Singh, S. K.; Yang, L.; Beal, M. F.; Goldman, S. A. Functional engraftment of human ES cell-derived dopaminergic neurons enriched by coculture with telomerase-immortalized midbrain astrocytes. Nat. Med. 12(11):1259–1268; 2006.
32. Song, P.; Xie, Z.; Guo, L.; Wang, C.; Xie, W.; Wu, Y. Human genome-specific real-time PCR method for sensitive detection and reproducible quantitation of human cells in mice. Stem Cell Rev. 8(4):1155–1162; 2012.
33. Teng, Y. D.; Benn, S. C.; Kalkanis, S. N.; Shefner, J. M.; Onario, R. C.; Cheng, B.; Lachyankar, M. B.; Marconi, M.; Li, J.; Yu, D.; Han, I.; Maragakis, N. J.; Llado, J.; Erkmen, K.; Redmond, D. E., Jr.; Sidman, R. L.; Przedborski, S.; Rothstein, J. D.; Brown, R. H., Jr.; Snyder, E. Y. Multimodal actions of neural stem cells in a mouse model of ALS: a meta-analysis. Sci. Transl. Med. 4(165):165ra164; 2012.
34. Uchida, N.; Buck, D. W.; He, D.; Reitsma, M. J.; Masek, M.; Phan, T. V.; Tsukamoto, A. S.; Gage, F. H.; Weissman, I. L. Direct isolation of human central nervous system stem cells. Proc. Natl. Acad. Sci. USA 97(26):14720–14725; 2000.
35. Yang, D.; Zhang, Z. J.; Oldenburg, M.; Ayala, M.; Zhang, S. C. Human embryonic stem cell-derived dopaminergic neurons reverse functional deficit in parkinsonian rats. Stem Cells 26(1):55–63; 2008.
36. Yasuhara, T.; Matsukawa, N.; Hara, K.; Yu, G.; Xu, L.; Maki, M.; Kim, S. U.; Borlongan, C. V. Transplantation of human neural stem cells exerts neuroprotection in a rat model of Parkinson's disease. J. Neurosci. 26(48):12497–12511; 2006.
37. Zhu, Q.; Ma, J.; Yu, L.; Yuan, C. Grafted neural stem cells migrate to substantia nigra and improve behavior in Parkinsonian rats. Neurosci. Lett. 462(3):213–218; 2009.